Appl Phys B (2010) 98: 61–67
DOI 10.1007/s00340-009-3735-1

Applied Physics B
Lasers and Optics

Nd:YAG lasers at 1064 nm with 1-Hz linewidth

Y. Jiang · S. Fang · Z. Bi · X. Xu · L. Ma

Received: 19 April 2009 / Revised version: 9 July 2009 / Published online: 19 September 2009

Abstract Two Nd:YAG lasers are tightly frequency-stabilized to separately located, vertically mounted ultrastable cavities, which are connected by single-mode optical fibers employing fiber phase noise cancellation. The optical heterodyne beat between two independent lasers shows that the linewidth of each laser reaches 1 Hz and the frequency drift is less than 0.3 Hz/s.

PACS 42.55.Px · 42.60.Da · 42.62.Eh · 06.30.Ft

1 Introduction

Spectrally narrow lasers are required in optical atomic clocks, high-resolution laser spectroscopy, measurements of fundamental constants, and tests of fundamental physics [1–8]. Most lasers available have broad spectral linewidths on the order of kHz or even MHz due to fast phase fluctuations. To suppress phase noise, a laser can be frequency-locked to an ultrastable optical reference cavity with high finesse by using the Pound-Drever-Hall (PDH) technique [9]. Profiting from the length stability of the reference optical cavity, the laser linewidth can be significantly reduced to the Hz level [10–14]. With this kind of narrow linewidth lasers, several clock transitions of cold atoms are observed with linewidths of a few Hz [14–21].

In our early work [22], two Nd:YAG lasers at 1064 nm were servo-locked to two separated vertically mounted optical cavities, and the linewidth of each laser reached 2 Hz. In this work, we have made improvements on these cavity-stabilized Nd:YAG lasers. Temperature stabilization for electro-optic modulators (EOM), fiber phase noise cancellation, and light intensity stabilization were implemented on the experimental setup. With these improvements, the laser is tightly frequency-stabilized to the ultrastable reference cavity. The optical heterodyne beat between two independent cavity-stabilized lasers with the same configuration shows that the linewidth (FWHM, full width at half maximum) of each laser reaches 1 Hz and the frequency drift is reduced to less than 0.3 Hz/s.

Y. Jiang · S. Fang · Z. Bi · X. Xu · L. Ma (✉)
State Key Laboratory of Precision Spectroscopy, East China Normal University, Shanghai 200062, China
e-mail: lsma@phy.ecnu.edu.cn
Fax: +86-21-62233215

2 Experimental setup

In this work, the laser source to be stabilized is an Nd:YAG laser operating at 1064 nm (Innolight OEM 200NE). By using the PDH technique, the laser frequency is servo-locked to an ultrastable, Fabry-Perot (FP) cavity with a length of 77.5 mm and a finesse of nearly 300,000. The length stability of reference cavities is an important contribution to the frequency stability and linewidth of cavity-stabilized lasers. Since environmental noise modulates cavity length, the cavity has to be well designed and isolated from external perturbations.

As shown in Fig. 1, the reference cavity, which is made of ULE (ultralow expansion) glass with a shape like an American football, is vertically supported by three Teflon posts at its mid-plane, specially designed to minimize fluctuations of the cavity length due to environmental perturbations [11]. To reduce radial forces in the cavity spacer due to thermal expansion of the support structure, the Teflon posts rest in holes of a ULE ring, since ULE has an ultralow thermal expansion coefficient. This kind of cavity was designed by JILA [14] and is commercially available from Advanced

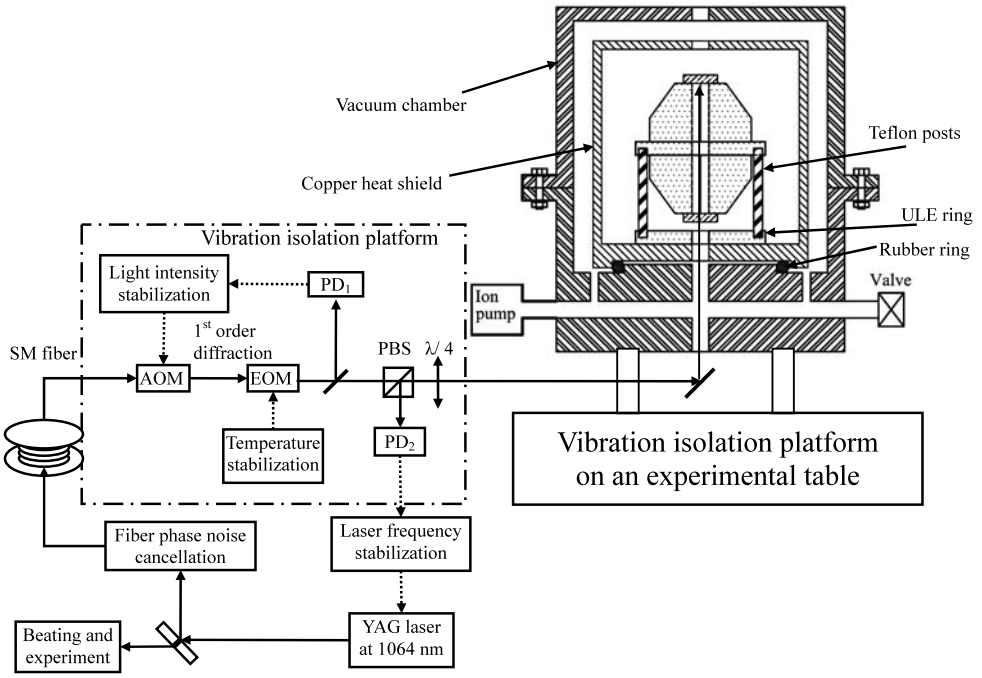

Fig. 1 Schematic diagram of the experimental setup. AOM: acousto-optic modulator; EOM: electro-optic modulator; PBS: polarization beam splitter; $\lambda/4$: quarter-wave plate; SM fiber: single-mode fiber; PD: photodetector

Thin Film [23]. Then the cavity, together with the posts and the ULE ring, are heat-shielded in a gold-coated copper cylinder to achieve a homogenous thermal environment. The copper heat shield is sitting inside a vacuum chamber on a piece of soft rubber ring for damping and thermal isolation. The whole vacuum chamber is evacuated to $\sim 10^{-7}$ mbar by a 20 L/s ion pump, which is located at the bottom of the vacuum chamber to prevent direct heat radiation from the ion pump onto the ULE cavity (see Fig. 1). Two temperature controllers are separately employed for homogenous temperature stabilization of the vacuum chamber, which is made of aluminum alloy for better thermal conductivity. To reduce the thermal influence of environmental perturbations, the whole chamber is wrapped in thermal insulation. Good temperature stabilization and thermal insulation yield a temperature instability of less than 1.5 mK at $\sim$28 °C in a 12-h measurement.

Moreover, the reference cavity and parts of optical components are isolated from low-frequency vibrations with a BM-4 bench top vibration isolation platform from Minus K technology. Nevertheless, some part of acoustic noise can fluctuate cavity length through air and cables. Therefore the whole experimental setup is enclosed by a foam screen to reduce the direct influence of both air flow and acoustic transmission, and all the cables are suspended with springs and rubber bands. Unfortunately, some cables, especially those of the ion pumps and the lasers, are too stiff to prevent vibration coupling. Correspondingly, we replace the power supply cable of the ion pump with a softer one. As for the laser cable, we place the laser head outside the vibration isolation platform that holds the reference cavity. By using a single-mode (SM) optical fiber, laser light can be easily transferred to the vibration isolation platform.

On the vibration isolation platform, the light is frequency-shifted by an acousto-optic modulator (AOM) for optical isolation. Then the first-order diffraction beam passes through an EOM to generate sidebands beside the laser carrier frequency by optical phase modulation. The temperature of the EOM is stabilized above room temperature with a fluctuation of less than 0.1°C to reduce the influence of residual amplitude modulation (RAM) [24, 25]. The light reflected from the reference cavity is steered onto a photodetector (PD_2) by a combination of a quarter-wave plate ($\lambda/4$) and a polarization beam splitter (PBS). The PD_2 detects the optical beat signal between the carrier and the sidebands reflected by the reference cavity. Then the beat signal from the PD_2 is mixed down to get the frequency discrimination signal, which is used to control a piezoelectric transducer (PZT) bonded on the monolithic Nd:YAG crystal of the laser for laser frequency stabilization to the reference cavity. The servo bandwidth is about 44 kHz by analyzing servo error signals.

3 Fiber phase noise cancellation

Optical fiber provides mechanical flexibility to transfer optical beams. However, it will cause some problems: the optical phase and polarization of laser light transferred through the optical fiber are extremely sensitive to the environmental perturbations like pressure, temperature, etc. When laser light with 1-Hz linewidth is transferred through an optical

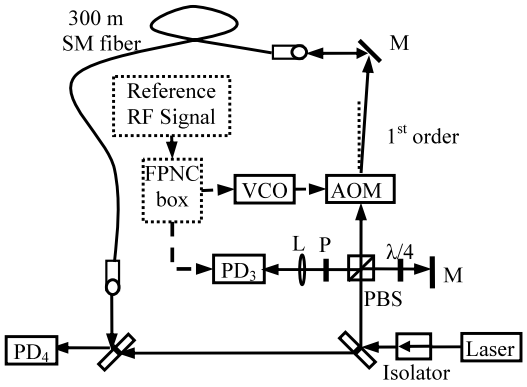

Fig. 2 Schematic diagram of the experimental setup for fiber phase noise cancellation (FPNC). AOM: acousto-optic modulator; PBS: polarization beam splitter; L: lens; $\lambda/4$: quarter-wave plate; P: polarizer; M: mirror; SM fiber: single-mode fiber; PD: photodetector

fiber, environmental perturbations will induce phase noise onto the light. As a result, the light suffers from a random phase modulation, and its linewidth after transfer is broadened. To maintain the phase coherence and narrow linewidth of the laser light, active fiber phase noise cancellation is required [26–29].

A schematic diagram of fiber phase noise cancellation is shown in Fig. 2. The light is split into two beams by a PBS, a short path located before an AOM and a long path containing the AOM and a SM fiber. The light in the short path, as a local signal, is directly reflected by a mirror and passes through the PBS by going through a quarter-wave plate ($\lambda/4$) twice. The light beam in the long path is frequency-upshifted ν_{AOM} by the AOM and then makes one trip through the fiber where fiber phase noise $e^{\mathrm{i}\phi}$ is written on. At the far end of the fiber, which is polished flat and normal, a portion of the light is reflected back through the fiber and the AOM, with a total frequency shift of $2 \times \nu_{\mathrm{AOM}}$ and a phase noise of $e^{2\mathrm{i}\phi}$. Some of the light is then reflected by the PBS and beats with that from the short path on a fast photodetector (PD_3) to generate a beat signal around $2 \times \nu_{\mathrm{AOM}}$. This beat signal, where the fiber-induced phase noise is encoded on, is then sent to a fiber phase noise cancellation (FPNC) electronic box to compare with a stable reference RF signal from a frequency synthesizer to extract a servo error signal. The servo error signal is then applied on a VCO (voltage-controlled oscillator) to correct the fiber-induced phase noise. Then the output signal of the VCO is frequency-divided by a factor of 2 and amplified to drive the AOM for cancellation of the fiber-induced phase noise.

To test the performance of fiber phase noise cancellation, a self-heterodyne method is used in Fig. 2. A SM fiber with a length of 300 m is employed (without any jacket and nearly open to the environment). A beat note centered at ν_{AOM} is obtained at a photodetector (PD_4) by heterodyning between the fiber input and output light. Figures 3a and 3b show linewidths of the beat notes without and with active cancellations accordingly, observed on a high resolution fast-Fourier-transform (FFT) spectrum analyzer (SR770). Without active phase noise cancellation, the linewidth of the beat note is 20.2 Hz when the resolution bandwidth (RBW) of the FFT spectrum analyzer is 7.8 Hz, but, when active fiber phase noise cancellation is applied, the linewidth reduces to 1.1 mHz, which is limited by the resolution of the FFT spectrum analyzer. Interestingly, we put the fiber in a tough environment where a fan as a perturbation source is turned on. Without active cancellation the linewidth of the beat note is broadened to the kHz level as shown in Fig. 3c. However, as soon as fiber phase noise cancellation is applied again, the beat note dramatically becomes narrower and its linewidth reaches 2.5 mHz, as shown in Fig. 3d. These results show that active phase noise cancellation can effectively cancel fiber-induced phase noise, and it helps to maintain coherence between the fiber input and output light.

4 Intensity stabilization

Besides phase noise introduced by optical fibers, polarization is also extremely sensitive to environmental perturbations. When laser light is transferred through the fiber to the vibration isolator platform, a polarizer will convert polarization noise into amplitude noise. With a 4-m-long fiber relative intensity fluctuation is measured to be as large as 10%. The fluctuation of the input power directly results in a variation of the cavity length and so does the laser frequency which is locked to the cavity. The intensity-dependent laser frequency shift is measured to be ~63 Hz/μW with an input light power of about 50 μW. If the laser frequency shift is expected to be controlled within 0.3 Hz/s, the relative amplitude fluctuation of input light should be controlled within 1×10^{-4} per second with the same input power. Therefore active intensity stabilization is critically important.

Implementation of light intensity stabilization is quite simple. As shown in Fig. 1, the power of the cavity input light is monitored by a photodetector (PD_1). This DC signal is then compared with a stable reference voltage to get an error signal. After a loop filter, the error signal modifies the drive power of the AOM to servo the light power. As a result, the relative intensity instability is reduced to 6.5×10^{-5} (1 s).

5 Results and discussion

To explore the frequency stability and linewidth of the laser, we have built two laser systems with the same design and independently stabilized to two ultrastable reference cavities. The laser light is sent to the vibration isolation platform

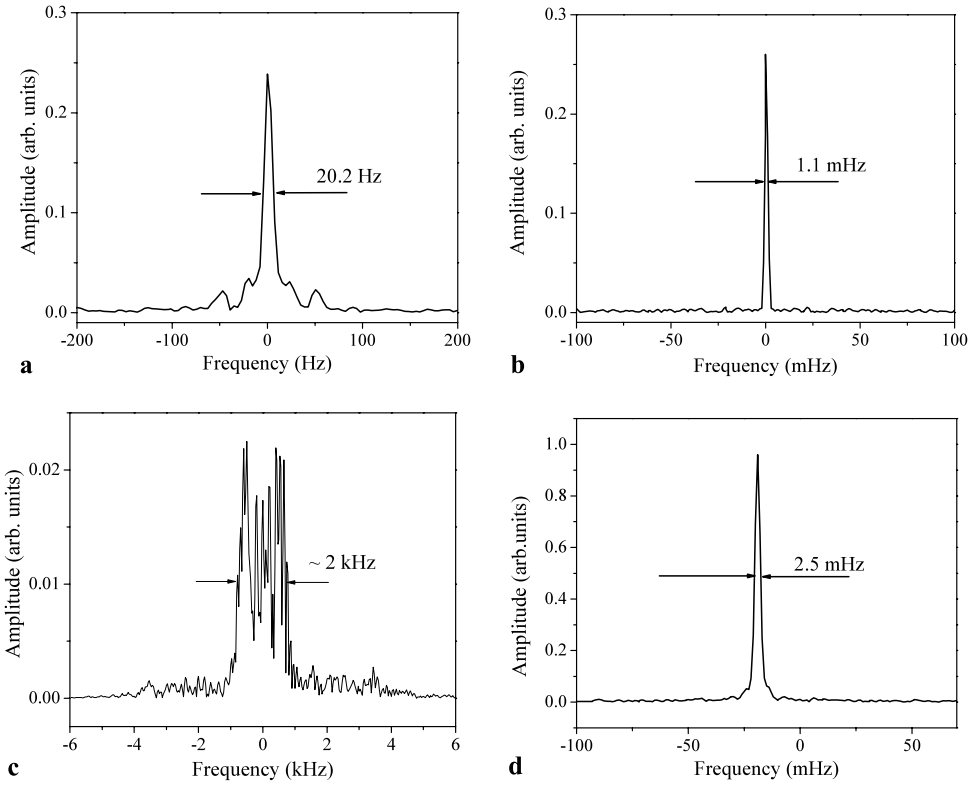

Fig. 3 Heterodyne beat signals between the fiber input and output light: (**a**) linewidths without active cancellation (RBW = 7.8 Hz) and (**b**) with active cancellation (RBW = 0.95 mHz); (**c**) linewidths without active cancellation (RBW = 32 Hz) and (**d**) with active cancellation (RBW = 0.95 mHz) when a fan as a perturbation source is turned on

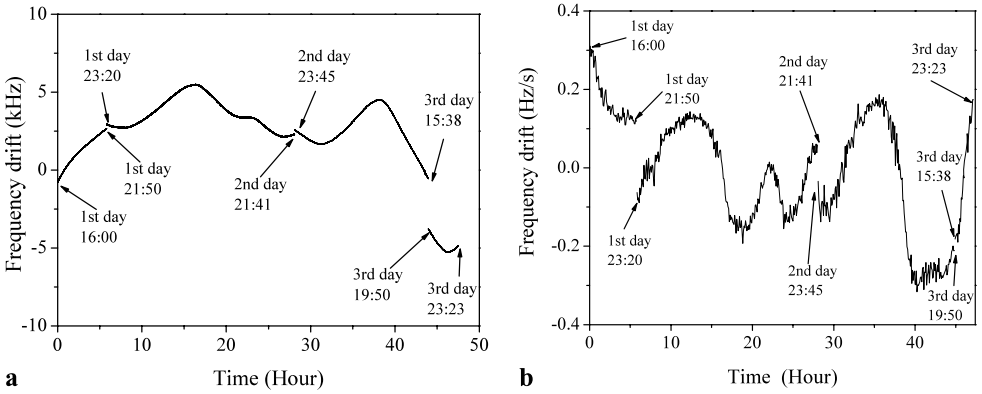

Fig. 4 (**a**) Frequency drift and (**b**) calculated frequency drift rate of the heterodyne beat between two cavity-stabilized lasers in three days. It was interrupted by linewidth measurements on each day

through a SM fiber with a length of 4 m. Both of the systems are equipped with fiber phase noise cancellation and intensity stabilization. The frequency of the beat note between the two laser systems was detected on a photodetector and counted by a digital counter which communicates with a computer.

We measured the relative frequency drift of the beat note in three days, only interrupted by linewidth measurements on each day, as shown in Fig. 4a. It drifts within 10 kHz over 47 h. Figure 4b shows the calculated frequency drift rate based on Fig. 4a. The frequency drift stays within ±0.3 Hz/s over this time. The laser frequency drift was not linear. In 40% of total 47 h the frequency drift was less than 0.1 Hz/s. An analysis of experimental results shows that temperature stability of the vacuum chamber is one of the key to reducing the frequency drift of the frequency-stabilized lasers. However, there is still a small laser frequency drift since the cavity temperature might not be stabilized at the temperature of the zero thermal-expansion coefficient of the ULE.

The fractional Allan deviation of the beat note is calculated and shown in Fig. 5. This measurement was taken directly by counting the heterodyne beat. And a linear laser frequency shift was removed by a linear fit to the data. Theoretical estimate of the thermal noise limited instability is shown as a solid horizontal line at 1×10^{-15}.

Figure 5 shows that at averaging time of 1 s the instability of the laser is slightly bigger than the thermal noise limited instability, which might be some vibration or acoustic noise applied on the vacuum chamber. However, at several seconds, the instability is pretty close to that of the thermal

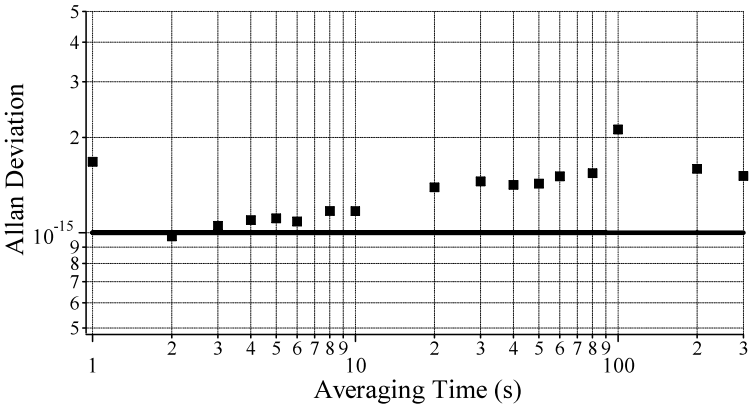

Fig. 5 Fractional Allan deviation of the stabilized laser frequency. Linear laser frequency drift was removed by a linear fit to the data. A *solid line* denotes the thermal noise stability limit of the reference optical cavity, which is near a fractional frequency stability of 1×10^{-15}

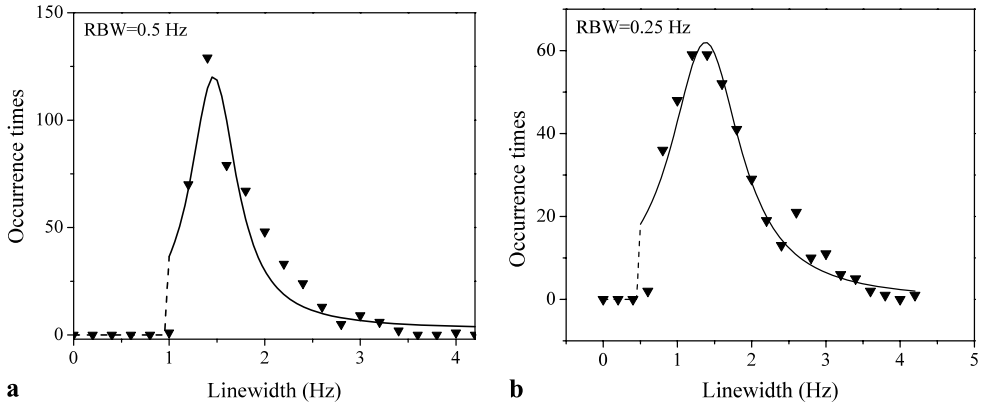

Fig. 6 Linewidth measurements over 11 days when the RBW of the FFT spectrum analyzer is set at (**a**) 0.5 and (**b**) 0.25 Hz. And the corresponding expected linewidths are 1.46 and 1.39 Hz, respectively. Linewidth measurements of the beat note between two frequency-stabilized lasers are shown with *triangle markers*, and their distributions are fitted with *solid lines*. There is a cutoff at almost twice the RBW of the FFT spectrum analyzer

noise limit, which might be corrected by removing the linear drift term. At a relatively long timescale, the instability gets bigger due to residual frequency drifts.

To measure the linewidth, the beat note between the lasers was mixed down to nearly 20 kHz with a RF signal from a synthesizer. And it was observed on a FFT spectrum analyzer which took data automatically according to a computer program and without any drift compensation of the beat frequency.

We made linewidth measurements over 11 days when the RBW of the FFT spectrum analyzer was set at 0.5 and 0.25 Hz. respectively, as shown in Figs. 6a and 6b. Each linewidth data is acquired by Lorentzian fitting the spectrum data obtained from the FFT spectrum analyzer. Figure 7 shows two samples of the beat note (dot) and its Lorentzian fit (solid line). In Fig. 7a, it shows a typical linewidth of the beat signal between two lasers is 1.5 Hz with the RBW of 0.5 Hz. When the RBW reduces to 0.25 Hz, a sub-hertz linewidth can be observed as shown in Fig. 7b. Figure 6 shows that the linewidth distribution deviates from normal distribution because there is a cutoff at nearly twice the resolution bandwidth of the FFT spectrum analyzer. Taking RBW = 0.5 Hz as an example, there is less possibility for linewidth observed to be less than 1 Hz due to the limitation of the resolution bandwidth. When the RBW is 0.25 Hz, sub-Hertz beat notes can be observed, as shown on Figure 6b. Statistical analysis of the observed data shows that the expected linewidths with the RBW of 0.5 and 0.25 Hz are 1.46 and 1.39 Hz, respectively. Therefore the linewidth of each laser reaches 1 Hz under the assumption that both stabilized lasers have the same linewidth.

In the linewidth measurements, acquisition time T_{acq} of each measurement increases as the resolution bandwidth of the FFT spectrum analyzer decreases. Therefore any frequency drift of the frequency-stabilized lasers in T_{acq} will result in a broadened linewidth known as drift-induced linewidth broadening. In this work, we measured the linewidth with both RBW = 0.5 Hz and RBW = 0.25 Hz, and the corresponding acquisition times were 2 and 4 s, respectively. In the experiment, the frequency drift kept within ±0.3 Hz/s, hence the maximum drifts in the acquisition times were 0.6 and 1.2 Hz, respectively. It is obvious that the drift-induced linewidth broadening might cause perceptible influence on the measurements with RBW =

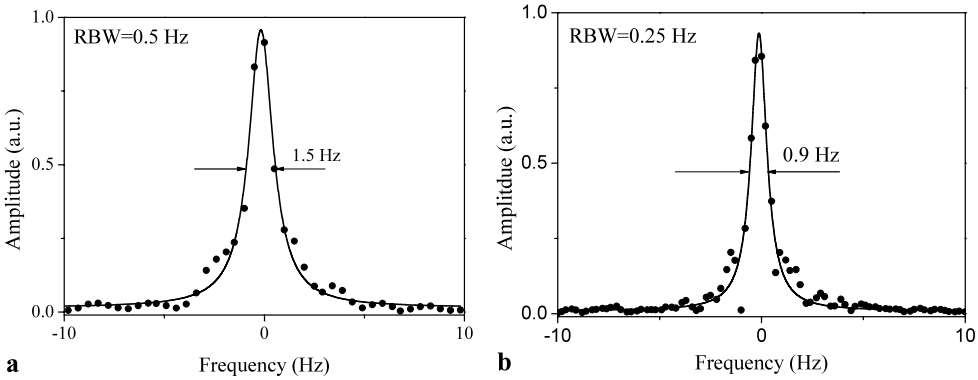

Fig. 7 Beat notes between two frequency-stabilized lasers (*dot*) and their Lorentzian fits (*solid line*) with the RBW of (**a**) 0.5 and (**b**) 0.25 Hz, respectively

0.25 Hz, while it is not the case with RBW = 0.5 Hz. Therefore when frequency drift is further reduced, linewidth measurement could be improved.

On a relatively long timescale, taking 10 s as an example, laser frequency drift can be removed by applying a feedforward frequency correction to an AOM [14]. Improvement of the length stability of the reference cavity is a direct and effective way to improve the laser frequency instability and linewidth as well. (1) Light intensity fluctuation might be a source to make cavity length unstable. Therefore, a better intensity stabilizer is required. (2) To reduce the effect of the room temperature fluctuation on the vacuum chamber another temperature-controlled box outside the vacuum chamber might be needed as well to improve the temperature stability. (3) Some experiments show that the temperature of the zero thermal-expansion coefficient of the ULE may be below room temperature [30, 31]. To explore that temperature point, we plan to make improvements on the next step by applying Peltier elements to control the temperature of the vacuum chamber. This will enable us to determine the temperature of zero thermal-expansion coefficient of the cavities even below room temperature and to further reduce the temperature fluctuations of the ULE reference cavities. (4) An acoustic isolation chamber can effectively reduce acoustic noise by as much as 40 dB, which will help to reduce perturbation of the cavity length and thus the laser frequency that is stabilized to it. (5) Furthermore, even when we make the cavity insensitive to the thermal fluctuation and vibration noise mentioned earlier, and reduce RAM perfectly, thermal noise of the reference cavity is another important problem that limits the frequency stability of this kind of laser at 10^{-15}, which has drawn more attention recently [32, 33]. It results from Brownian thermal-mechanical noise, which occurs since there is $kT/2$ energy per degree of freedom in any mechanical system like cavity spacing, mirror substrate and coating. Calculations show that the flat thermal noise floor decreases when increasing mirror separation and optical mode diameter. They also suggest that it is possible to gain an improvement by a factor of 2 by trying a different substrate material [33].

6 Conclusion

Two Nd:YAG lasers are independently servo-locked to separately located, ultrastable cavities connected by optical fibers. With fiber phase noise cancellations and light intensity stabilization, the linewidth of each laser is 1 Hz and the frequency drift of the laser is less than 0.3 Hz/s.

Acknowledgements The authors wish to thank Jun Ye's group in JILA for significant help in building up the experimental setup. This work is supported by the National Natural Science Foundation of China (60490280 and 10774044), the National Basic Research Program of China (2006CB806005), the Science and Technology Commission of Shanghai Municipality, China (07JC14019), Shanghai Pujiang Talent Program of China (07PJ14038), and the Program for Changjiang Scholars and Innovative Research Teams and Shanghai Leading Academic Discipline Project (B408).

References

1. J.L. Hall, Rev. Mod. Phys. **78**, 1279 (2006)
2. T.W. Hänsch, Rev. Mod. Phys. **78**, 1297 (2006)
3. S.A. Diddams, T. Udem, J.C. Bergquist, E.A. Curtis, R.E. Drullinger, L. Hollberg, W.M. Itano, W.D. Lee, C.W. Oates, K.R. Vogel, D.J. Wineland, Science **293**, 825 (2001)
4. M.M. Boyd, A.D. Ludlow, S. Blatt, S.M. Foreman, T. Ido, T. Zelevinsky, J. Ye, Phys. Rev. Lett. **98**, 083002 (2007)
5. A.D. Ludlow, T. Zelevinsky, G.K. Campbell, S. Blatt, M.M. Boyd, M.H.G. Miranda, M.J. Martin, J.W. Thomsen, S.M. Foreman, J. Ye, T.M. Fortier, J.E. Stalnaker, S.A. Diddams, Y.L. Coq, Z.W. Barber, N. Poli, N.D. Lemke, K.M. Beck, C.W. Oates, Science **319**, 1805 (2008)
6. C.W. Hoyt, Z.W. Barber, C.W. Oates, T.M. Fortier, S.A. Diddams, L. Hollberg, Phys. Rev. Lett. **95**, 083003 (2005)
7. T.M. Fortier, N. Ashby, J.C. Bergquist, M.J. Delaney, S.A. Diddams, T.P. Heavner, L. Hollberg, W.M. Itano, S.R. Jefferts, K. Kim, F. Leve, L. Lorini, W.H. Oskay, T.E. Parker, J. Shirley, J.E. Stalnaker, Phys. Rev. Lett. **98**, 070801 (2007)
8. R.S. Conroy, Contemp. Phys. **44**, 99 (2003)
9. R.W.P. Drever, J.L. Hall, F.V. Kowalski, J. Hough, G.M. Ford, A.J. Munley, H. Ward, Appl. Phys. B **31**, 97 (1983)
10. B.C. Young, F.C. Cruz, W.M. Itano, J.C. Berguist, Phys. Rev. Lett. **82**, 3799 (1999)
11. M. Notcutt, L.S. Ma, J. Ye, J.L. Hall, Opt. Lett. **30**, 1815 (2005)
12. H. Stoehr, F. Mensing, J. Helmcke, U. Sterr, Opt. Lett. **31**, 736 (2006)

13. S.A. Webster, M. Oxborrow, P. Gill, Opt. Lett. **29**, 1497 (2004)
14. A.D. Ludlow, X. Huang, M. Notcutt, T.Z. Willette, S.M. Foreman, M.M. Boyd, S. Blatt, J. Ye, Opt. Lett. **32**, 641 (2007)
15. N. Poli, Z.W. Barber, N.D. Lemke, C.W. Oates, L.S. Ma, J.E. Stalnaker, T.M. Fortier, S.A. Diddams, L. Hollberg, J.C. Berquist, A. Brusch, S. Jefferts, T. Heavner, T. Parker, Phys. Rev. A **77**, 050501(R) (2008)
16. R.J. Rafac, B.C. Young, J.A. Beall, W.M. Itano, D.J. Wineland, J.C. Bergquist, Phys. Rev. Lett. **85**, 2462 (2000)
17. T. Rosenband, P.O. Schmidt, D.B. Hume, W.M. Itano, T.M. Fortier, J.E. Stalnaker, K. Kim, S.A. Diddams, J.C.J. Koelemeij, J.C. Bergquist, D.J. Wineland, Phys. Rev. Lett. **98**, 220801 (2007)
18. J. Stenger, C. Tamm, N. Haverhamp, S. Weyers, H.R. Telle, Opt. Lett. **26**, 1589 (2001)
19. Th. Becker, J.V. Zanthier, A.Yu. Nevsky, Ch. Schwedes, M.N. Skvortsov, H. Walther, E. Peik, Phys. Rev. A **63**, 051802(R) (2001)
20. P. Dube, A.A. Madej, J.E. Bernard, L. Marmet, A.D. Shiner, Appl. Phys. B **95**, 43 (2009)
21. T. Rosenband, D.B. Hume, P.O. Schmidt, C.W. Chou, A. Brusch, L. Lorini, W.H. Oskay, R.E. Driullinger, T.M. Fortier, J.E. Stalnaker, S.A. Diddams, W.C. Swann, N.R. Newbury, W.M. Itano, D.J. Wineland, J.C. Bergquist, Science **319**, 1808 (2008)
22. Y.Y. Jiang, Z.Y. Bi, X.Y. Xu, L.S. Ma, Chin. Phys. B **17**, 2152 (2008)
23. R. Lalezari, Advanced Thin Films, Longmont, CO, USA
24. E.A. Whittaker, M. Gehrtz, G.C. Bjorklund, J. Opt. Soc. Am. B **2**, 1320 (1985)
25. N.C. Wong, J.L. Hall, J. Opt. Soc. Am. B **2**, 1527 (1985)
26. L.S. Ma, P. Jungner, J. Ye, J.L. Hall, Opt. Lett. **19**, 1777 (1994)
27. J. Ye, J.L. Peng, R.J. Jones, K.W. Holman, J.L. Hall, D.J. Jones, S.A. Diddams, J. Kitching, S. Bize, J.C. Bergquist, L.W. Hollberg, L. Robertsson, L.S. Ma, J. Opt. Soc. Am. B **20**, 1459 (2003)
28. S.M. Foreman, A.D. Ludlow, M.H.G. Miranda, J.E. Stalnaker, S.A. Diddams, J. Ye, Phys. Rev. Lett. **99**, 153601 (2007)
29. I. Coddington, W.C. Swann, L. Lorini, J.C. Bergquist, Y.L. Coq, C.W. Oates, Q. Quraishi, K.S. Feder, J.W. Nicholson, P.S. Westbrook, S.A. Diddams, N.R. Newbury, Nature Photonics **1**, 283 (2007)
30. J. Alnis, A. Matveev, N. Kolachevsky, Th. Udem, T.W. Hänsch, Phys. Rev. A **77**, 053809 (2008)
31. S.A. Webster, M. Oxborrow, S. Pugla, J. Millo, P. Gill, Phys. Rev. A **77**, 033847 (2008)
32. K. Numata, A. Kenmery, J. Camp, Phys. Rev. Lett. **93**, 250602 (2004)
33. M. Notcutt, L.S. Ma, A.D. Ludlow, S.M. Foreman, J. Ye, J.L. Hall, Phys. Rev. A **73**, 031804 (2006)